



## PERFORMANCE ASSESSMENT OF THREE-STORY SHAPE MEMORY ALLOY REINFORCED CONCRETE WALLS

Emad A. Abraik

Ph.D. Candidate. Civil and Environmental Engineering, Western University, London, ON, N5X 3P3, Canada

Maged A. Youssef

Professor. Civil and Environmental Engineering, Western University, London, ON, N5X 3P3, Canada

### ABSTRACT

The need for sustainable structures, that provide adequate ductility without experiencing major damage, has led researchers to develop methods to achieve self-centering structures. One of these methods involves the use of superelastic Shape Memory Alloy (SMA) bars. This study assesses the seismic performance of a three-story SMA Reinforced Concrete (RC) shear wall considering different potential locations for the SMA bars. The maximum inter-story drift, residual drift, and damage scheme are evaluated using Incremental Dynamic Analysis (IDA). The use of SMA bars at the plastic hinge of the first floor was found to significantly reduce the residual drifts and associated damage.

Keywords: Concrete shear walls, SMA, incremental dynamic analysis, inter-story drift ratio, residual drift

### 1. INTRODUCTION

Superelastic shape memory alloy (SMA) is a unique material that has the potential to improve the seismic performance of civil structures. The attractive features for this alloy are self-centering after large inelastic deformations and corrosion resistance.

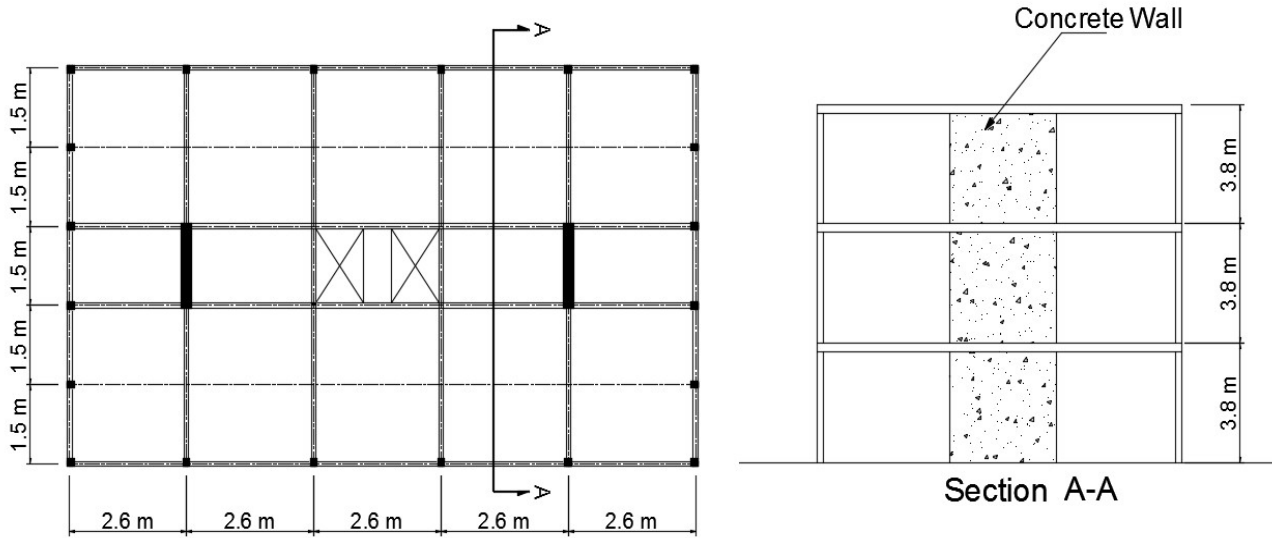
The use of SMA as a passive vibration damper in a cable-stayed bridge was analytically investigated by Sharabash and Andrawes (2009). SMA dampers successfully controlled the bridge seismic behaviour. Saiidi et al. (2008) highlighted the improved ductility and reduced residual displacements for RC bridge columns having SMA bars in their plastic hinge zone. The efficiency of utilizing SMA bars in near-field ground motion was analytically assessed by DesRoches and Delemont (2002). Their experimental study included simply-supported and multi-span bridges that utilize SMA restrainers, which significantly reduced the bridge deck response and the relative hinge displacement. The cyclic performance of an RC beam–column joint that utilized SMA bars at plastic hinge zone was experimentally investigated by Youssef et al. (2008). The results showed significant recovery of inelastic deformations.

Abdulridha (2012) experimentally studied the cyclic behaviour of an RC wall that utilized SMA bars in the plastic hinge region. The SMA bars increased the wall ductility and reduced the residual displacements. Effendy et al. (2006) used external SMA bars to improve the seismic performance of existing squat walls. The test results showed a significant reduction in residual displacements combined with 16% to 26% increase in the peak shear strength. Abraik and Youssef (2015) conducted an analytical study to identify the performance of SMA RC squat and intermediate walls considering different SMA bar locations. The results highlighted that the SMA bars location has a significant effect on the wall residual drifts.

This paper describes the seismic behaviour of three-story RC SMA walls. IDA results of maximum inter-story drifts and residual drifts are utilized to evaluate the seismic response. The results of the SMA RC walls were compared to a conventional RC wall. It was found that the SMA RC walls achieved reliable seismic performance over the conventional RC wall.

## 2. BUILDING DESCRIPTION

A three-story prototype reinforced concrete building located in Vancouver, BC, was designed. The building has a 13 m by 7.5 m floor plan and a height of 11.4 m. The lateral resisting system is composed of two shear walls in the transverse direction and moment resisting frames in the longitudinal direction as shown in Figure 1. The modelled wall was designed according to the 2010 National Building Code of Canada with total force reduction factor of 5.6. Figure 2 shows the shear walls reinforcement details.



(a) Floor Plan

(b) Section A-A

Figure 1. Three-Story Building

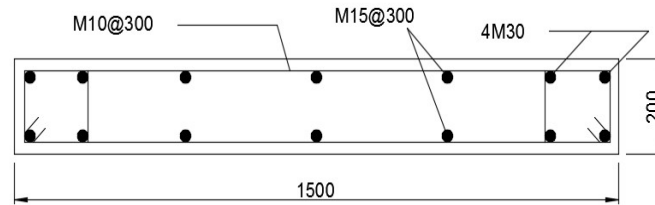


Figure 2. Wall Cross Section Details

## 3. SEISMIC GROUND MOTIONS

Table 1 summarizes important information about the chosen ground motions. Scaling of the ground motions was based on the Mean Square Error (MSE) (PEER, 2015; Michaud and L ger, 2014). The method minimizes the error between the spectral acceleration of the record and the target spectrum, which was chosen to be the uniform hazard spectrum for Vancouver, BC. Figure 3 shows the spectral acceleration of chosen ground motions scaled to the site design spectrum assuming 5% damping.

Table 1. Ground motion parameters

Motion	Title	Duration (Sec)	PGA (g)
San Fernando	ORR021 ORR291	61.81	0.29
Imperial Valley-06	H-CPE147 H-CPE237	63.82	0.16
Irpinia Italy-01	A-CTR000 A-CTR270	35.21	0.14
Corinth Greece	COR—L COR--T	41.32	0.24
Loma Prieta	CYC195 CYC285	40.00	0.13
Northridge-01	GLE170 GLE260	30.00	0.15
Cape Mendocino	LFS270 LFS360	28.68	0.25

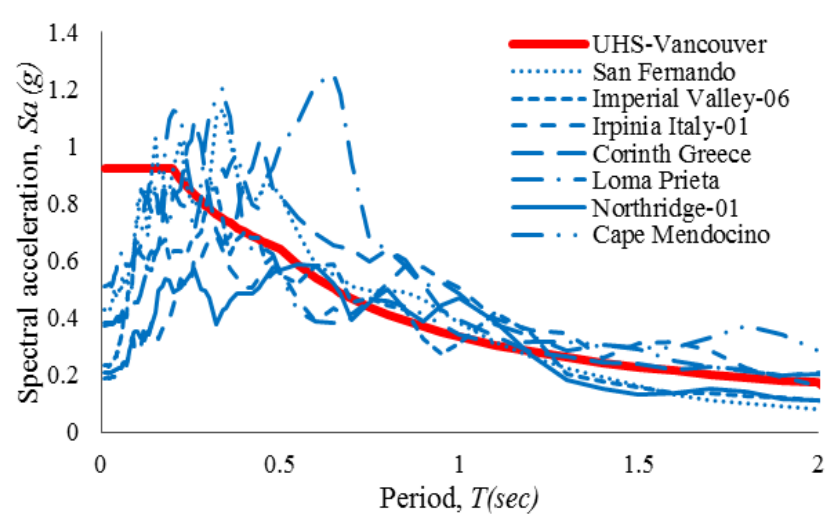


Figure 3. Spectral Acceleration of the Chosen Ground Motions

#### 4. ANALYTICAL MODELING

The Shear Flexural Interaction Multi-Vertical Line Element (SFI-MVLE) proposed and validated by Kolozvari (2013) was selected for this study. The stress-strain relationships proposed by Chang and Mander (1994), Menegotto and Pinto (1973), and Christopoulos et al. (1973) to model the behaviour of concrete, steel bars, and SMA bars, respectively, were adopted. Table 2 shows the properties of the SMA reinforced. The SFI-MVLEM is relatively simple, numerically stable, and provides an accurate prediction of axial-flexural and shear-flexural interaction for moderate and slender walls.

Each MVLE consists of six degrees of freedoms. They represent the horizontal deformation, the vertical deformation, and the rotation at the top and bottom of the element. Two-dimensional membrane RC panels, Figure 4, are utilized to capture the flexural and shear behaviour of the RC wall. The shear resistance along the cracks is accounted for using a fixed angle approach.

The relative rotation between the top and bottom faces of the wall element is assumed to occur at 40% of the element's height (Kolozvari, 2013). The flexural response of the wall is captured through the axial deformation of the RC panels in the vertical direction. The average vertical and shear strains can be determined by dividing the average vertical or shear deformation by the element height. The strain in the horizontal direction is obtained by dividing the horizontal deformation at the internal degrees of freedom of the element by the panel width.

Failure was assumed when the global drift capacity is reached, which is defined by FEMA 355F (2000) as the drift at which the slope of the IDA is less than 20% of the elastic range slope or at which the analysis terminates because of numerical instability (flat line).

Table 2. Material properties of the SMA

Properties	Title
Yield Strength	380 (MPa)
Modulus of Elasticity	38000 (MPa)
Maximum Strain	7%
Maximum Stress	500 (MPa)

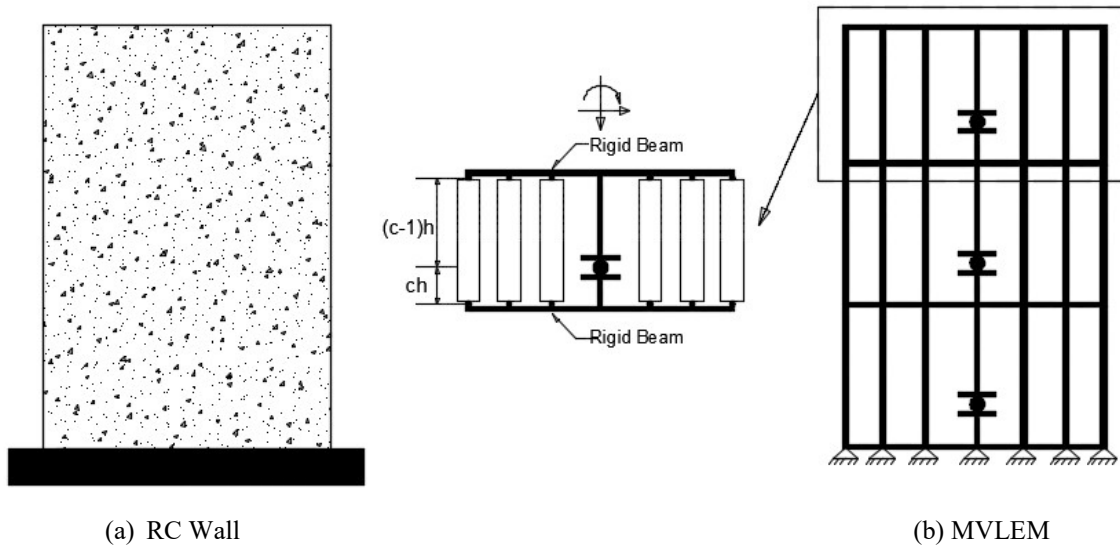


Figure 4. Modeling the 3-Story Shear Wall

## 5. EIGENVALUE ANALYSIS

Figure 5 shows the considered cases that are SMA bars at the plastic hinge of the first floor (PF), SMA bars at the plastic hinge of the first and second floor (PFS), SMA bars at the plastic hinge of first, second, and third Floor (PFST). The 1<sup>st</sup> and 2<sup>nd</sup> time periods for the analyzed walls are shown in Figure 6. The fundamental period of SMA RC walls was larger than the RC wall by 9% on average.

## 6. INCREMENTAL DYNAMIC ANALYSIS

The IDA curves represent the relationship between the Engineering Demand Parameter (EDP) and the Intensity Measure (IM) for a set of suitably selected ground motions. The mean, 84%, and 16% fractiles are shown in Figure 7. It is clear that structural resurrection happened in Figures 7a, 7b, and 7d. The steel RC wall exhibited a flat-line at PGA of 0.91g corresponding to 5.0% and 3.6% maximum inter-story drift for the 84% and 50% fractiles, respectively. Utilizing SMA bars on each floor (PFST wall) led to delaying failure to 1.04g considering 84% of the records. The analytical results show that all SMA RC walls experienced higher maximum inter-story drifts compared with the RC wall.

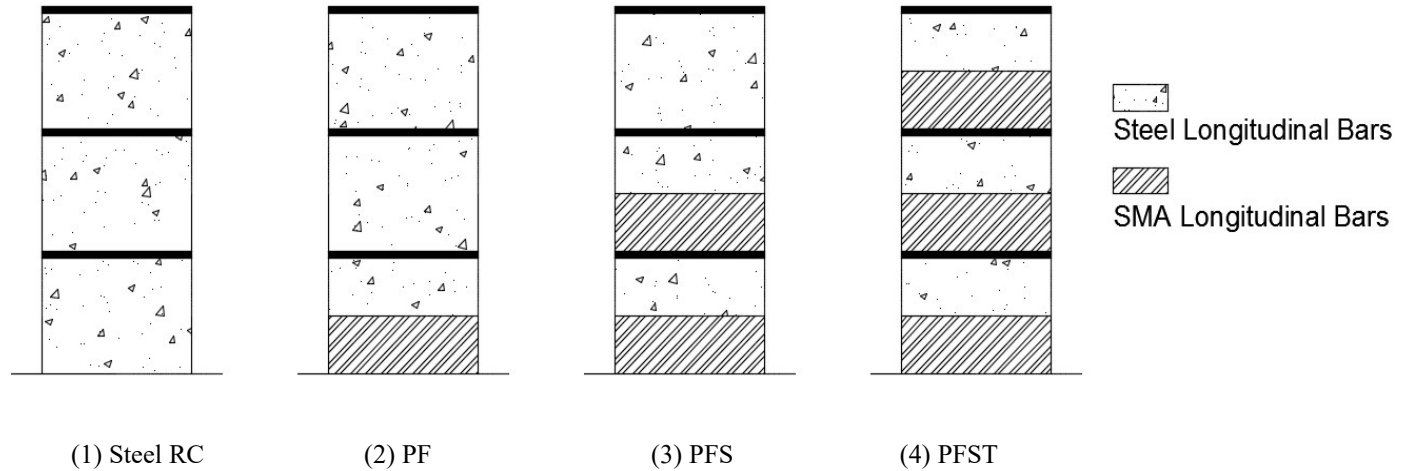


Figure 5. Analyzed walls

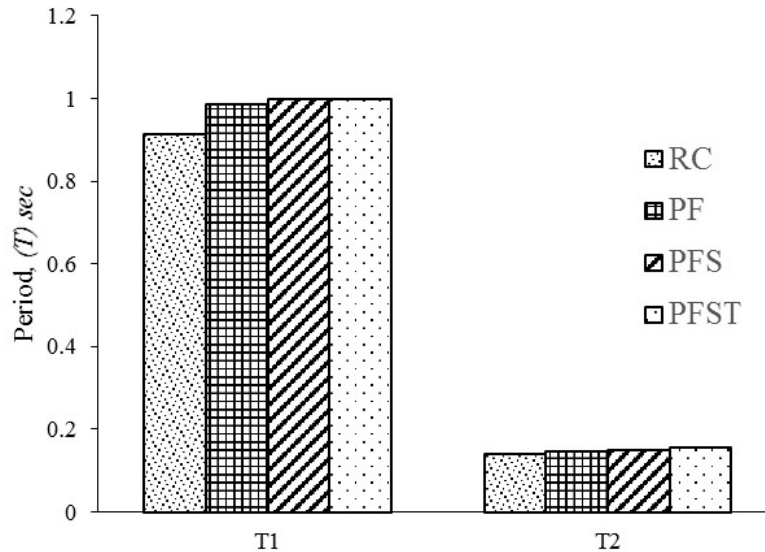


Figure 6. Eigenvalue analysis

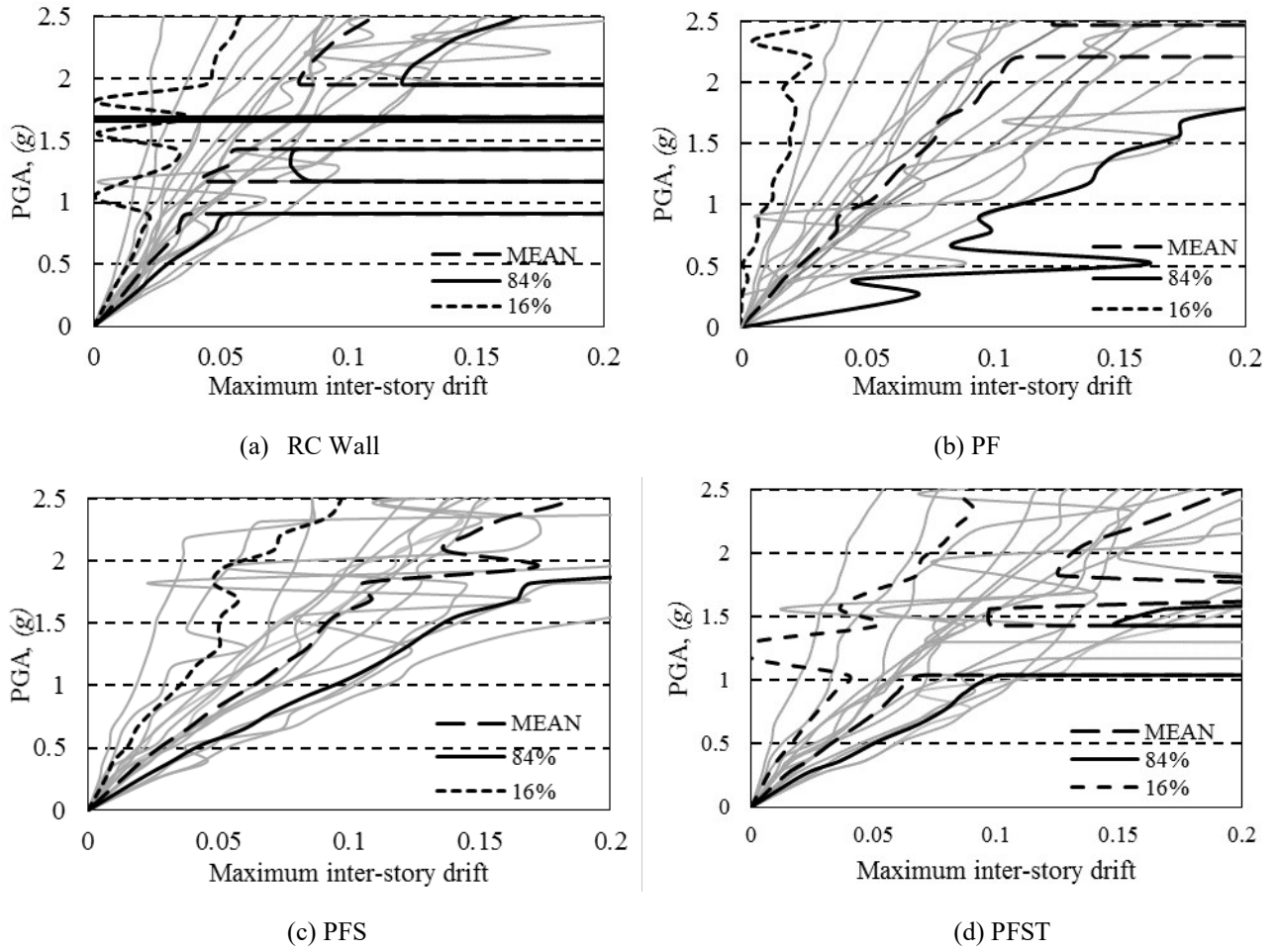


Figure 7. Maximum inter-story drift

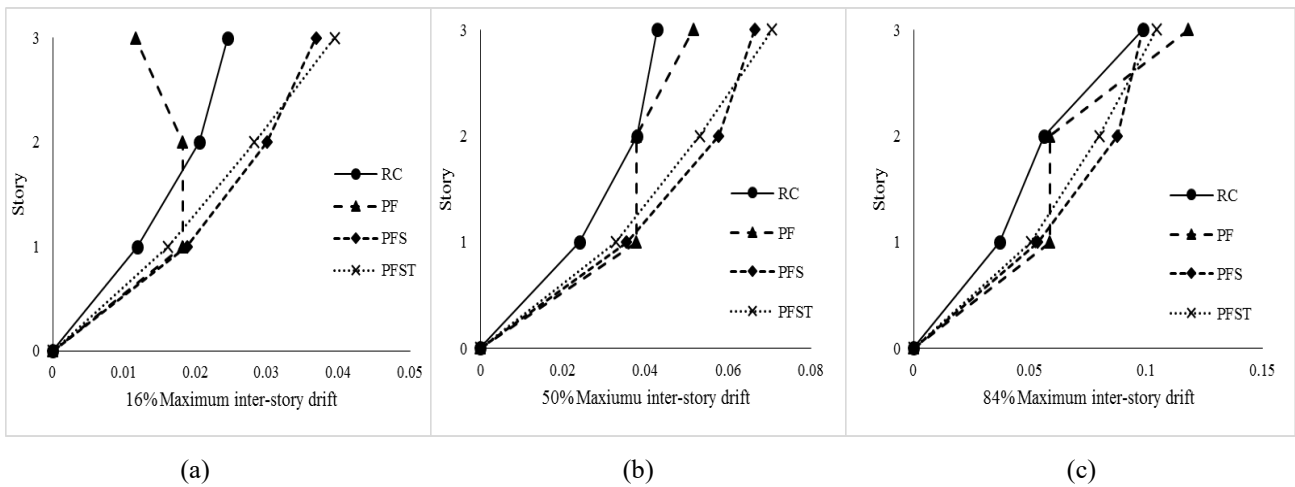
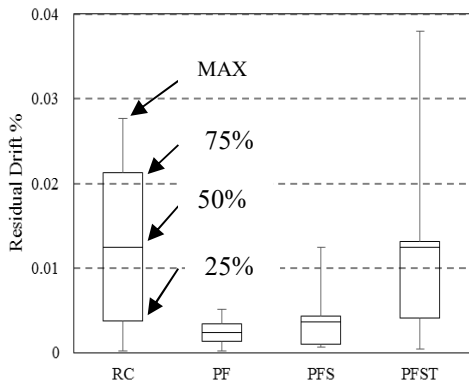
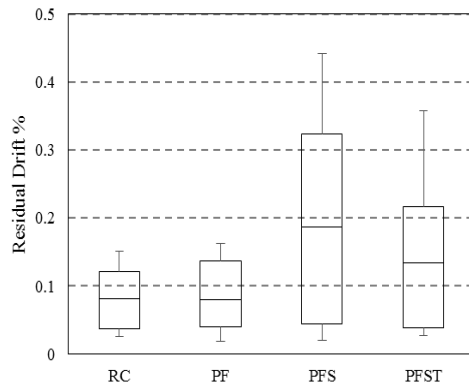


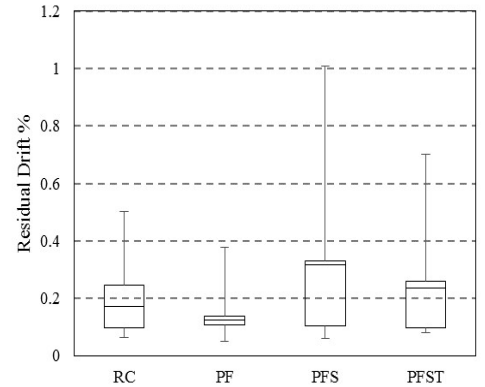
Figure 8. Story drift demand



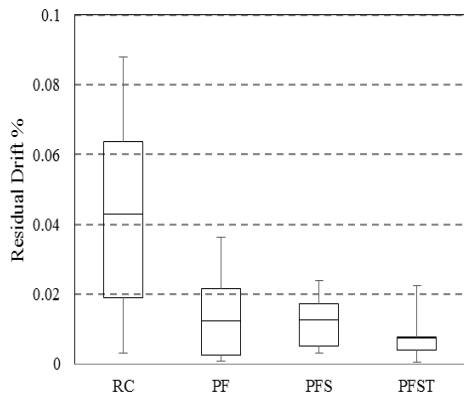
(a) 16% First Story



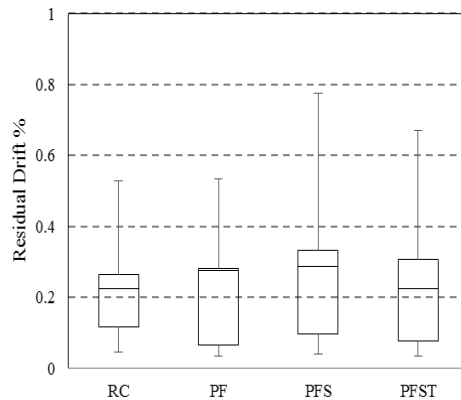
(b) 50% First Story



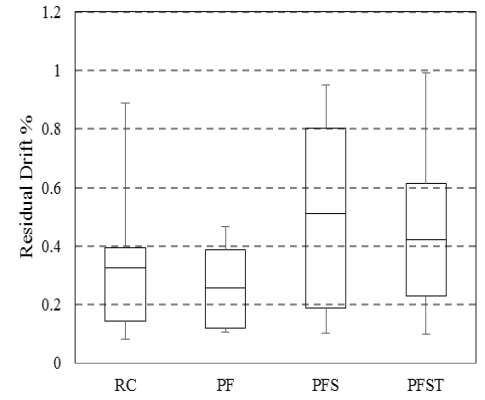
(c) 84% First Story



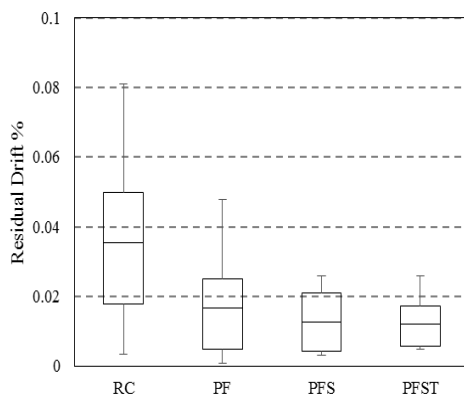
(d) 16% Second Story



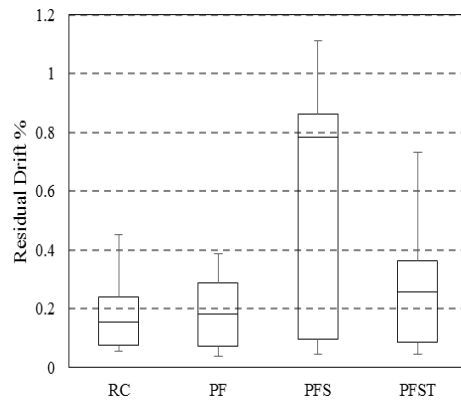
(e) 50% Second Story



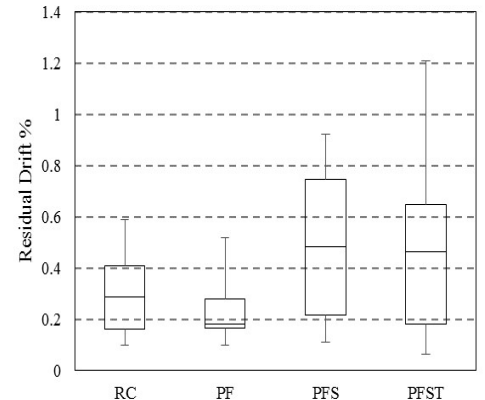
(f) 84% Second Story



(g) 16% Third Story



(h) 50% Third Story



(i) 84% Third Story

Figure 9. Residual drift at 0.91g PGA

## 7. MAXIMUM INTER-STORY DRIFT RESULTS

Figure 8 presents the maximum story drift for all cases at 0.91 PGA for 16%, 50%, and 84% fractiles. The use of SMA bars increased the inter-story drift for the first floor by 39% on average for all fractiles. The inter-story drift for the second story did not change when SMA bars were used at first floor (PF). The inter-story drift increased by 53% and 41% on average when the SMA bars were also used in the third and/or second stories (PFS, PFST). The drift of the third-story increased by 9%, 25%, and 29% for PF, PFS, and PFST, respectively.

## 8. RESIDUAL DRIFT RESULTS

The residual drifts were calculated for different fractiles at each story and are shown in Figure 9. Each plot illustrates the maximum, mean (50%), and minimum, as well as the 75% and 25% marks for the data. Although the residual drifts of the PFS and the PFST cases appear to be high at the first story for 50% and 84% fractiles, both walls recovered about 98% of the maximum inter-story drift. The results of the PF wall at first floor exhibited lower residual drifts for all fractiles.

The second story had slightly increased residual drifts for all fractiles as compared to the first floor. The results of 84% fractiles show that even so the inter-story drift reached 51% in the second story, the residual drift does not exceed 0.5%, 0.9%, and 1% for The PF, PFS, and PFST, respectively. The residual drifts for 50% of the data at the first and second stories do not exceed 0.2% and 0.3% considering all cases, respectively. The PF case showed lower residual drift as compared with the other cases (Figures 9d, 9e, and 9f).

The results of 16% fractiles at third story showed that all SMA cases have almost the same average of 0.015% residual drift. Whereas the maximum values for both PFS and PFST are equal. A rapid change in the behaviour is noted in Figure 9h and 9i. Residual drifts for 50% and 75% of the data for the PF case are slightly higher than the case of RC wall. However, the maximum residual drift for the PF case is smaller than that for the RC wall case. For 50% and 84% fractiles data, both PFS and PFST exhibited higher residual drifts.

## 9. CONCLUSION

Four three-storey RC walls were assessed using IDA analysis. The analytical study intended to investigate enhancing the performance of RC walls by considering several SMA bars locations within multi-storey RC walls. Eigenvalue analysis was conducted for all considered cases and the results showed that the SMA wall fundamental period increases by an average of 9%.

The RC wall exhibited the first structure resurrection phenomena at 0.91g followed by the PFST case, which failed at 1.04g. For the PF case, 50% of the records produced a flat line at 2.2g.

The inter-story drift results of PF case was generally less than other SMA wall cases and it was concluded that using the SMA bars at first story increased the inter-story drift by 39% and 9% for the first and third stories, respectively. However, there does not seem to be any obvious trend with the peak drift in the second story.

Limiting the use of the SMA bars at the plastic hinge of the first floor is considered as an efficient sustainable design due to the significant recovery in the inter-story drift along the building height.

## 10. REFERENCES

- Abdulridha, A. 2012. "Performance of Superelastic Shape Memory Alloy Reinforced Concrete elements subjected to monotonic and cyclic Loading," *Ph.D. Thesis, University of Ottawa, Ottawa*.
- Abraik, E., Youssef, M.A. 2015. "Cyclic Performance of Shape Memory Alloy Reinforced Concrete Walls," *Fifth International Workshop on Performance, Protection & Strengthening of Structures under Extreme Loading*, No. 5, pp. 326-333.
- Chang G A., Mander J B. 1994. "Seismic Energy Based Fatigue Damage Analysis of Bridge Columns: Part I Evaluation of Seismic Capacity" NCEER Technical Report No. NCEER-94-0006, State University of New York, Buffalo, N.Y.
- Christopoulos, C., Tremblay, R., Kim, H.-J., Lacerte, M. 2008. "Self-Centering Energy Dissipative Bracing System for the Seismic Resistance of Structures: Development and Validation". *Journal of Structural Engineering ASCE*, 134(1), 96-107.
- DesRoches, R. Delemont, M. 2002. "Seismic Retrofit of Simply Supported Bridges Using Shape Memory Alloy," *Engineering Structures*, Vol. 24, No. 3, pp. 325-332.
- Deng, Z., Li, Q., Sun, H. 2006. "Behavior of Concrete Beam with Embedded Shape Memory Alloy Wires," *Engineering Structures*. Vol. 28 Issue 12, pp. 1691-1697.
- FEMA 355 F (2000). "State of the Art on Performance Prediction and Evaluation of Steel Moment-Frame Buildings," Federal Emergency Management Agency, Washington, D.C.
- Effendy, E., Liao, W., Song, G., Mo, Y., Loh, C. 2006. "Seismic Behavior of Low Rise Shear Walls with SMA Bars," *Earth & Space*. Vol.3, pp. 1-8.
- Kolozvari K. 2013. Analytical Modeling of Cyclic Shear – Flexure Interaction in Reinforced Concrete Structural Walls. *PhD Dissertation*, University of California: Los Angeles.
- Menegotto, M., Pinto, P.E. 1973. "Method of analysis of cyclically loaded RC plane frames including changes in geometry and non-elastic behavior of elements under normal force and bending". Preliminary Report IABSE, vol 13.
- Michaud, D., Lèger, P. 2014. "Ground motions selection and scaling for nonlinear dynamic analysis of structures located in Eastern North America," *Canadian Journal of Civil Engineering*, Vol. 41, No. 3, pp. 232-244.
- NRCC. 2010. National Building Code of Canada; Part 4: Structural Design. National Research Council of Canada, Ottawa, ON, Canada.
- Pacific Earthquake Engineering Research (PEER) 2015 ground motions database available online: <http://ngawest2.berkeley.edu/>
- Saiidi, S., O'Brien, M., Sadrossadat-Zade, M. 2008. "Cyclic Response of Concrete Bridge Columns Using Superelastic Nitinol and Bendable Concrete," *ACI Structural Journal*, Vol. 106, No. 1, pp. 69-77.
- Sharabash, A.M., Andrawes, B., 2009. "Application of Shape Memory Alloy Dampers in the Seismic Control of Cable-Stayed Bridges," *Engineering Structures*, Vol. 31, No. 2, pp. 607-616.
- Youssef, M.A, Alam, M.S., Nehdi, M., 2008, "Experimental Investigation on the Seismic Behaviour of Beam-Column Joints Reinforced with Superelastic Shape Memory Alloys," *Journal of Earthquake Engineering*, Vol. 12, No. 7, pp.1205-1222.